C.3

DEPARTMENT OF MINERALS AND ENERGY

BUREAU OF MINERAL RESOURCES, GEOLOGY AND GEOPHYSICS

Record 1976/8

MADANG (PNG) 1974 GEOPHYSICAL SURVEY

by

B.H. Dolan, C.L. Horsfall, and E.J. Polak

Record 1976/8

MADANG (PNG) 1974 GEOPHYSICAL SURVEY

by

B.H. Dolan, C.L. Horsfall, and E.J. Polak

CONTENTS

SUMMARY

Gamma logging, resistivity depth probing, and seismic refraction surveys were carried out by the Bureau of Mineral Resources, Geology and Geophysics in the Madang area of Papua New Guinea. The purpose of the surveys was to investigate the fresh-water and saline aquifers in the town area, and to test the presence of building sand and gravel deposits in the Gogol River valley.

Thirty-two resistivity depth probes were measured using a Schlumberger electrode arrangement with spacing AB up to 600 m. The depth probes indicate that the unconsolidated deposits above the bedrock are of non-uniform composition with large lateral changes. The presence of salt water is indicated on many of the resistivity depth probes; the thickness of the fresh water lens becomes small towards the shore line. Measurements of resistivity of water from bores and surface water were also carried out to aid in interpretation.

Gamma-ray logging of 5 bores indicates the layering in the unconsolidated sediments, but no correlation between bore logs is possible.

Six seismic refraction spreads in the Gogol River valley indicated that sand and gravel exist as a thin layer overlying very thick deposits of mixed clay, silt, and sand. No large deposits of clean sand and gravel were located.

1. INTRODUCTION

Madang is on the north coast of Papua New Guinea (Plate 1) at 05°13'S and 145°48'E, and is the main town of the Madang District, an area of 25 600 km^2 with a population of more than 200 000. The population of Madang Town was 16 000 in 1971. Detailed statistics are not available, but the process of urban drift is continuing, with large numbers of people leaving villages to work in Madang (JIO, 1972). To provide work for these people industrialization is advancing quickly, making Madang the main port for this part of New Guinea and the centre of commerce and industrial activities based on fishing, timber logging and processing, boat building and repairing, and other activities. All these activities require additional supplies of water and construction materials.

The high rainfall, averaging 3547 mm per year, generally provides the water supply for domestic use. The industrial water and supplementary domestic supply come from shallow wells which provide hard but potable water. Over-pumping of these wells may introduce salt water encroachment especially during the dry season.

At the request of the Geological Survey of Papua New Guinea a survey was carried out by the Bureau of Mineral Resources, Geology and Geophysics (BMR). The purpose of the survey was to determine the distribution and thickness of the freshwater aquifer overlying the salt water and to determine the quality and quantity of sand and gravel deposits in the bed of the Gogol River.

The survey was carried out between 4 July and 20 July 1974 by a party consisting of B.H. Dolan, C.L. Horsfall, and E.J. Polak, geophysicists from the Engineering Group of BMR, R.B. Moana, a geophysicist from the Geological Survey of Papua New Guinea, and four field hands provided by the Public Works Department. Topographical surveying was arranged by the Department of Lands, Surveys and Mines.

2. MADANG GROUNDWATER SURVEY

Although the town is served by several perennial rivers and streams, which provide generally an abundant supply of water throughout the year, the town depends generally on tank water supplemented with underground water. During an exceptional long, dry spell the rivers stop flowing and the encroachment of the sea water is noticeable. These dry spells occur mostly between July and September.

2-1 Geology and Hydrology

Geology. Madang is located on the extensive Quaternary deposits consisting of alluvial, beech, and sedimentary rocks of the Wandakai Limestone Formation (Macias, 1972).

Alluvial and beach deposits are present in rivers and creeks and along the sea shore. The alluvium along the rivers and creeks consists of gravel and sand, mostly of volcanic origin. Beach deposits along the coast consist of green sand of volcanic origin or of coral and shell debris.

Coral limestone crops out in the coastal plain and in rivers and creeks west of Madang. In the Madang area the coral limestone forms a flat surface occasionally distorted with terraces, sinkholes, and remnants of reefs.

At many localities coral limestone is overlain with silty clay deposits. These deposits may be interbedded with the coral limestone. The maximum thickness of the overlying clay was found to be 2.5 m.

Hydrology. From the examination of borehole evidence (Macias, 1972) the main aquifers in the area are either in the coral limestone or in coral debris and gravels. The lateral extension of the aquifer may be very limited. Several aquifers are unconfined; others are confined artesian, and lie at a depth of 6 to 30 m. Several of each type were proved by boring.

Fresh water from the coral limestone aquifers is of good quality, but many unconfined aquifers are biologically polluted. Where the initial supply was satisfactory the bores were fully developed. Supplies from these bores range from 4000 to 18000 litres per hour. Some of the bores struck salt water.

Plate 2 shows the location of bores and wells which were used in the interpretation of geophysical data.

2-2 Gamma-ray logging of boreholes

Gamma-ray logging was used at Madang, where five water-bores were logged. The purpose of the test was to determine whether the gamma logging can distinguish clay from other types of rocks. Generally the radioactivity of clay and shale is several times that of the other types of common sedimentary rock and sand owing to their high potassium content. The increase in gamma-ray intensity is nearly proportional to the increase in the clay content of a rock.

Gamma-ray logging can be used in open and cased bore-holes, whether full of water, drilling mud, or empty.

Plate 3 shows the gamma logs obtained during the survey. Letters A to F in Plate 2 indicate the positions of the wells in which the logs were obtained.

The geological log of bore no. 227 (Macias, 1972), which is near bore 286 in which log "C" was run, shows 'yellow clay' to a depth of 1.8 m followed by 'blue clay' and 'fine coral limestone sand (water-bearing)'. The gamma log indicates a decrease in radioactivity at a depth of 2 m followed by low radioactivity to a depth of 6 m, then a gradual increase with depth. This gradual increase in radioactivity is noticeable on the other four logs and may indicate that the clay content in the rocks increases with depth.

Twelve samples of water were also collected from bores and lagoons. The resistivities of the water samples were measured (Table 1) in a mud cell, and from the resistivities the equivalent NaCl concentrations were calculated.

Table 1 - Salinity and resistivity of water sample, Madang

Map Symbol	Location	Resistivity (ohm-metres)	Salinity (ppm NaCl)
A	Technical School bore	210	30
B	" " "	1.9	3100
C	Airport Bore	25.4	220
D	" "	23.3	260
E	Baidal Rd, Komoklon Cr. bore	-	-
F	Yabob; Baidal Road bore	-	-
G	Kasagten Road Well	12.7	480
H	Yamauan St lake	34	160
I	" " "	25.4	220
J	Sea Inlet, Yamauan St	0.26	+15 000
K	" " "	0.27	+15 000
L	Golf Course Lake	29.6	180

2-3 Resistivity depth probing

The basic principles of resistivity depth probing and the relation of the resistivity of the rock to the quality of water enclosed in rocks were discussed by Dolan et al. (1975).

The same equipment was used in this survey with the Schlumberger electrode arrangement. The interpretation was done using the same methods: that is comparison with precalculated standard curves (Compagnie Generale de Geophysique, 1955) and using the Hummel (1932) principle. The interpreted model curves were checked using either a Cyber 76 computer with a program developed by Zohdy (pers. comm.) or a program developed by the Engineering Geophysics Group of the BMR for a Wang 600 desk calculator.

Thirty-two depth probes were completed during the survey. The location of all depth probes is shown in Plate 2. The maximum distance between current electrodes is indicated as the length of the symbol on the plate. Normally the current electrodes were expanded to 600 m. The orientation of the symbol shows the direction in which the advance of electrodes was done.

Table 2 shows the results of interpretation of the resistivity depth probing. The results of interpretation are also shown in Plate 2 in the form of bar diagrams. The depths and resistivities indicated refer to the centre of each spread.

Table 2 indicates that in Madang the resistivity structure of the ground can be represented as three to five-layer model. Using the Hummel principle it is possible to reduce two near-surface layers into one equivalent layer, and introducing the bottom layer - the bedrock into the interpretation a four-layer model will be most commonly used in Madang.

The near-surface layer consists of soil, humus, coral debris, fill in the reclaimed areas, etc. The resistivities in this layer vary from 500 ohm m in dry coral debris down to 1.6 ohm m in wet mud at tidal creeks.

The second layer consists of the same rock as the near-surface but is generally saturated with water. The resistivities in this layer are considerably lower than the resistivities on the Kavieng survey, owing to a much higher content of clayey and silty material. Table 3 indicates the correlation between the resistivities of the layer models deduced from depth probing, and the data on water quality and depth from drilling of nearby bores (Macias, 1972). The interpreted resistivities of strata where fresh water entered the bore vary between 6 ohm m and 85 ohm m.

The third layer contains salt water. From experience on other surveys (Kavieng, Wewak, Ayr, Bowen, Moruya, Koo-weerup) the resistivity of rocks saturated with sea water is generally between 1 and 2 ohm m. The evidence from a comparison with the drilling data (Table 3) suggests that the

Table 2 - Madang - Resistivity Depth Probes

Depth Probe	Surface Elevation	Top Layer r1	h_1	2nd Layer r2	h_2	3rd Layer r3	h_3	4th Layer r4	h_4	5th
1	5.30	500	3	26	18	1.5	(half Schlumberger)			
2	3.06	140	3	35	18	2				
3	6.93	75	.7	50	17	1.5	77	1000		
4	6.68	34	.6	1.8	1.2	28	29	1	90	1000
5	1.10	30	2	3	12	1				
6	2.37	300	1.2	33	12	1	52	2		
7	6.26	102	.7	238	7	6	20	1000		
8	3.97	16	.85	64	5.1	16	35	1	75	40
9	5.19	12	.8	25	5.3	1.2	55	20		
10	8.03	10	.8	25	1.2	10	10	1	19	8
11	4.74	15	1.1	1	1.2	15	20	5	80	1000
12	5.96	15	7.5	1.7	37.5	1000				
13	7.89	10	1.35	4.3	2.7	10	40	90		
14	3.55	60	.4	6.5	4.0	1				
15	4.97	9	4.6	36	40.6	3.8				
16	3.73	56	.6	150	3.0	6.3	52	1		
17	6.96	65	2.6	125	3.5	7.5	48	300	52	1
18	6.02	120	.85	340	6	38	38	1		
19	4.36	85	8	9	50	2				
20	16.17	7	17	27	65	1				
21	4.99	680	4	75	12	1.5				
22	2.91	180	8	4.6	48	1	78	1000		
23	5.88	270	7	30	42	2				
24	5.53	264	6.5	30	39	1				
25	6.74	75	1.6	175	10	4				
26	24.91	6	1.2	230	12	2.5				
27	12.12	200	.5	6	5.5	14	56	2		
28		100	.5	26	5.0	2.9				
29		150	1.9	37	25	10	232	1		
30	4.32	10	1	14	7.5	6.3	40	2.5	200	1000
31		280	.86	9	9	36	54	1.5		
32		126	.95	28	10	1.4	60	1000		

Table 3 - Comparison of resistivity and drilling data on water depth and quality

Depth Probe			Drilling		
No.	depth(m)	resist (ohm m)	No.	depth(m)	
4	1.2	22	142		
	29	28		25	fresh water in limestone, gravel, and clay
		1			
7	7	230	143		
	20	6		12	fresh water in coral limestone
		1000			
8	6	60		2	fresh water in coral limestone
	35	16			
		1			
9	5	25	227		
	55	1			
		20		46	fresh water in coral limestone
10	7	1.2	235		
	10	10		7	fresh water in coral limestone
		1			
14	4	6	104	2	water in limestone (hard but potable)
		1			
15	5	9	226		
	40	36			
		4		30	salty water in coral limestone
16	3	150	234	5	water
	52	6		34	small supply
		1			
18	6	340	256	5	water (potable)
	38	38			
		1			
19	8	85	259	4	fresh water
	50	9			
		2			
29	2	150	242		
	25	37			
	232	10			
		1		33	fresh water

rock of resistivity up to 6 ohm m may represent unconsolidated material saturated with salt water. There is no evidence of salt-water intrusions on probes nos. 7, 12, 13, and 15.

The fourth layer represents the bedrock. The bedrock on depth probes nos. 3, 4, 7, 11, 12, 22, 30, and 32 is of very high resistivity. The indicated 1000 ohm m is not the true resistivity of the bed; it is merely an indication that the rock is of very high resistivity representing relatively impervious low-porosity rocks. On several locations (depth probes nos. 8, 9, 10, 13, and 15) the fourth layer's resistivity is less than 80 ohm m. This resistivity may represent either weathered bedrock or older alluvium, and the depth of the fresh bedrock has not been reached owing to the expansion of the electrode spread being too short. Further expansion of electrodes was not required because the information sought lies within 50 m of the surface. In the resistivity depth probing using the Schlumberger arrangement the depth of investigation is about one-quarter of the current electrode spacing.

Plate 2 shows the interpretation of the resistivity data in form of bar diagrams. A cursory examination of the diagrams indicates several major points:

(i) The first-layer and second-layer resistivities differ from depth prove to depth probe, supporting the geological and gamma-logging evidence of the lack of the lateral continuity of the strata.

(ii) Most depth probes indicate the existence of a low-resistivity salt-water layer, and in general the depth to this layer is greatest on the probes farthest from the coast. The major exception is in the area between Bilcan Road and the aerodrome where the saline layer is very close to surface as indicated on three probes (9, 14, 28).

(iii) The depth to the salt-water layer varies greatly and does not support the simple concept of uniform overlying freshwater lens. This may result from the existence of low-permeability layers and the entry of salt water along tidal streams and their valleys.

(iv) Some depth probes, especially on the east coast of the peninsula, show high-resistivity bedrock.

Plates 4 to 8 show all the depth probes taken during the survey. The depth probes are grouped along traverses.

Depth probes nos. 5, 1, 3, 4, & 31 (Pl. 4)

These probes were located roughly along a line at distances increasing away from the sea shore. Depth probe no. 5 indicates a relatively dry near-surface layer (2 m thick) with a resistivity of 30 ohm m. This layer is coral limestone, containing some salts brought in by sea spray. The layer below with resistivity 3 ohm m represents rocks saturated with a mixture of fresh and salt water. The bottom layer (resistivity of 1 ohm m) represents salt water encroachment.

Depth probe no. 1 shows similar conditions with a considerable increase in resistivity above the salt water encroachment. There is a general trend in the increase in the depth to the salt water layer inland from depth probe no. 5. Depth probes nos. 3 and 4 indicate an uplift in the bedrock, and the depth probe no. 31 shows thickening of the second layer with a resistivity of 36 ohm m, which may indicate more clayey conditions but still containing fresh water.

Depth probes nos. 17, 15, 9, 10, 11, 12, and 13 (Pl. 5)

Depth probe no. 17 shows two layers of high resistivity, both of which may carry fresh water. There is a great similarity between depth probe no. 31 (Pl. 4) and depth probe no. 15. Depth probe no. 15 shows a possibility of fresh water from a layer having a resistivity of 36 ohm m. This probe will be mentioned again in discussion on probe no. 29 (Pl. 6). There is a change in the curve type between depth probes no. 15 and no. 9. Probe no. 9 is located close to Wagol River and there is an intrusion of salt water in the area as proved by bore no. 226. The intrusion did not reach bores nos. 227 and 286, as the bores produces potable water. The probes from nos. 10 to 13 are located close to the slopes of the range and indicate mostly weathered rock in situ, overlying high resistivity bedrock, but on depth probes nos. 10 and 11 there is evidence of saline water. The probe no. 13 could be affected by the Nagada River, which is not tidal in this section.

Depth probes nos 21, 7, 6, 2, 29, 28, 14, 32 (Pl. 6)

Depth probes nos. 21, 7, 6, and 2 indicate the intrusion of sea water at depth from 12 to 18 m and depth probe no. 7 also indicates the existence of bedrock close to the surface. It is possible that there is a local rise in bedrock, on which the peninsula was formed.

Depth probe no. 29 indicates a second layer with resistivity of 37 ohm m, much thicker than other probes. The probe is located close to bore no. 242 (drilled in the sea). The bore is flowing fresh water from a depth of 33 m.

It is suggested that bore no. 242, and depth probes nos. 29 and 15 (Plate 5) lie on the same structure bringing water from an outcrop in the west. This explanation is suggested because depth probes nos. 28 and 14 show different resistivity conditions, and no evidence of a freshwater horizon. Depth probe no. 32 indicates shallow fresh water overlying a low-resistivity layer, probably salt water, and the bedrock below. Bore-hole no. 104 produces hard but potable water from the depth of 4 m.

Depth probes nos. 22, 18, 19, 24, 16, 8, 17, 31, 30

All depth probes in the northeastern part of the traverse (nos. 22 to 16) show a three-layer resistivity model with resistivity values decreasing to the resistivity of salt water. Depth prove no. 24 has a second-layer resistivity of 30 ohm m, which may be high enough to indicate fresh water in a clayey environment. Depth probes nos 17 and 31 had been already discussed (Pls. 5 and 4). Depth probe no. 30 resembles other depth probes along the foothills of the ranges and indicates decreasing resistivity, but no clear indication of salt water is reached. At the depth of 200 m the high resistivity bedrock is indicated.

Depth probes nos. 23, 25, 26, 20 and 27 (Pl. 8)

Plate 8 shows the remaining 5 resistivity depth probes which were not included in traverses on Plates 4 to 7. Depth probes no. 23 is very similar to nos. 24 and 18 in the same area (Pl. 7). A high resistivity of 175 ohm m on depth probe no. 25 may indicate dry conditions.

Depth probe no. 26 is similar to nos. 25 and 22, indicating high near-surface resistivity associated with raised coastal cliff and underlying low-resistivity salt water. Depth probe no. 27 is similar to no. 31 (Pls 4 and 7) and no. 20 shows the features of depth probes no. 30 (Pl. 7), and 10 and 11, in Plate 5.

2-4 Conclusions

1. The resistivity survey indicates a very wide intrusion of salt water. Only four depth probes out of 32 do not show resistivities of 1 to 2 ohm m.

2. Lower resistivities met with in Madang suggest more clayey aquifers than in Kavieng.

3. The confined aquifers at depth, as located in bore no. 242 in Binnen Harbour, are very thin and therefore not amenable to direct location by the use of resistivity depth probing. They can be

located by association with less permeable strata (depth probes nos. 2, 9, and 15), which show higher resistivities resulting from fresh water invading them under pressure.

3. GOGOL RIVER SAND DEPOSITS

3-1 General. Two kinds of construction material are available in the Madang District (Macias, 1972; JIO, 1972).

(i) Coral limestone debris is common in the Gogol River mouth, at Assuar Mission, and north of Nagada Harbour. All these localities (Pl. 1) are a considerable distance away from the town of Madang. The material is suitable for road making, swamp-filling, etc.

(ii) Sand and gravel suitable for fill and road-making are also obtainable in large quantities from the alluvia of the local rivers such as Gum and Gogol. Good-quality sand for concrete work is not so plentiful and the Gogol River sand was found to be better in quality for this purpose. Therefore the investigation was concentrated in the Gogol River valley.

3-2 Geology. The Gogol river drains much of the south-east portion of the Adelbert Range. For most of its course it follows a narrow valley but about 40 km from the mouth of the river the flood plain widens.

The Adelbert Range consists mainly of basic to intermediate lava, lava breccia, tuffs, and volcanically derived sediments of Miocene and upper Oligocene age. In the southern part of the Range, argillite is the major rock.

In the area investigated the alluvium consists of 65 percent of volcanic rocks and 30 percent of intrusive rocks. Volcanic rocks include basalt, andesite, lithic tuff, and agglomerate. Intrusive rocks consist mostly of granodiorite, with some pegmatite and aplite. The remaining 5 per cent is of sedimentary origin. The size of particles varies from fine to 25 cm.

3-3 Methods and equipment. The seismic refraction method, which depends on the seismic velocity contrast between rock layers, was used in the survey. Unconsolidated rocks are characterized by low seismic velocities, the velocity depending on the degree of water saturation and the composition and size of particles. Weathered rocks show higher velocities, the velocity in unweathered rock depending on the constitution of the rock and its porosity.

The velocity in dry, near-surface rock may be lower or equal to the velocity in the air (330 m/s). With increase in compaction and moisture content the velocity increases. A velocity of 800 to 1000 m/s is common in near-surface rocks.

Below the water table the velocity of unconsolidated rock is generally above 1500 m/s, although the velocities may be as low as 800 m/s if the rocks contain a large proportion of clay. The upper limit of velocities in unconsolidated material not containing clay is much more difficult to define. It may reach 2600 m/s when the valley is filled by large blocks up to 1 m in diameter, but generally the maximum velocity is below 1800 m/s.

Five seismic spreads were shot along the highway and one in the river. The equipment used in the survey was a 12-channel seismic refraction set type SR4 manufactured by SIE Houston, Texas, USA.

Each seismic spread consisted of 12 geophones laid out in a straight line on the ground at 10, 15, or 19 m intervals. Explosive shots were fired at distances of 5, 100, and 200 m from each end of the geophone spreads and a photographic record was made of the arrival times of the shot energy at each geophone.

The arrival times at each geophone were plotted against distance from a shot to form a time-distance curve (Pl. 9, Inset). The plotting and calculations were done using a Wang 600 desk calculator and plotter. The apparent seismic velocity is equal to the reciprocal of the gradient of the best-fitting straight line plotted through the arrival times. The measured apparent velocity depends on the slope of the seismic interface; it is lower than the true velocity when the interface is sloping away from a shot to the geophones, and vice versa. The true velocity is then calculated from reversed profiles; the results are shown in the centre of the plot.

The depth to a seismic interface at each end of a seismic spread is obtained from the intercept times of the different velocities at the shot points (Heiland, 1946).

The time-distance curve shown in Plate 9 indicates a velocity of 1900 m/s on the downstream end of the spread overlying a thick bed of lower (820 m/s) velocity. The bed with velocity of 1900 m/s is gravel. This bed carries very little energy, indicating that it is thin.

3-4 <u>Results</u>. Plate 9 shows the results of the interpretation of seismic survey along the road, crossing the extensive flood plain. As no surface elevation values are available the profile is plotted with the ground surface level. Actually spread no. 6 was placed on a low ridge between the Gogol and Mura Rivers.

The structure indicated by the seismic survey consists of three layers.

The surface layer with a velocity of 300 to 400 m/s consists of a mixture of mud, humus, sand, and gravel above the water table.

The velocity in the second layer on spread no. 5 is only 820 m/s, indicating that the material here is similar to the surface layer but below the water table. The bed may contain thin layers of sand and gravel but mostly mud and clay. The velocity in this layer increases southwards to reach 1000 m/s on spread no. 2. This increase may indicate either a higher content of coarse particles or the presence of older, more compacted alluvium. In this section the third layer consists of very weathered rock. Fresh bedrock has not been reached with the shots fired 200 m from the end of spread no. 1, indicating that the depth to fresh bedrock is at least 150 m.

Spreads no. 3, 4, and 6 are probably located on an uplift in the bedrock, and the second layer probably consists of highly weathered rock as the velocity is too high for alluvium. Less weathered rock, showing a seismic velocity of 2100 m/s, was located on spread no. 3.

3-5 Conclusions

Seismic refraction work along the road south of the bridge on Gogol River indicates that the existence of large deposits of sand and gravel is very unlikely. Very thin lenses of sand and gravel are possible, but their location with the seismic refraction survey is not possible.

4. REFERENCES

DOLAN, B.H., HORSFALL, C.L., & POLAK, E.J., 1975 - Kavieng (New Ireland, PNG), 1974 - Resistivity depth probing. Bur. Miner. Resour. Aust Rec. 1975/63 (unpubl.).

COMPAGNIE GENERALE DE GEOPHYSIQUE, 1955 - ABAQUES DES SONDAGE ELECTRIQUE, Geophys. Prospecting 3., Suppl. 3.

HEILAND, C.A., 1946, GEOPHYSICAL EXPLORATION - N.Y., Prentice Hall.

HUMMEL, J.N., 1932 - A theoretical study of apparent resistivity in surface potential method. Trans. Am. Inst. Min. Met. Eng., 97, 392-422.

JIO, 1972 - PAPUA NEW GUINEA, MADANG DISTRICT, GENERAL REPORT. Canberra, Dep. Defence.

MACIAS, L.F., 1972 - Engineering geology of the Madang town area. Geol. Surv. PNG, Note Inv. 72-003.

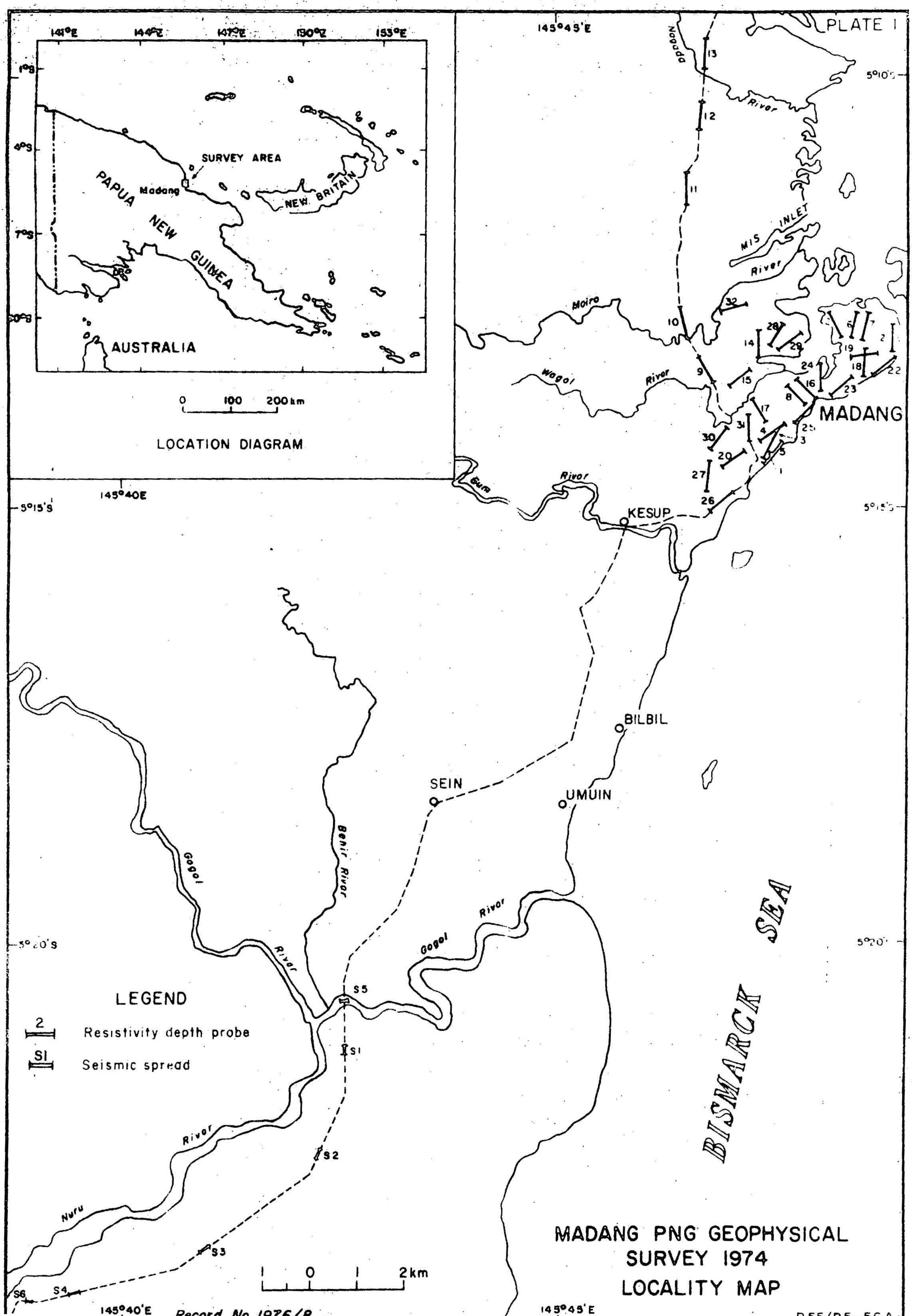

PLATE 1
LOCATION DIAGRAM
141°E
144°E
147°E
150°E
153°E
SURVEY AREA
Madang
PAPUA NEW GUINEA
NEW BRITAIN
AUSTRALIA
0 100 200 km
145°45'E
145°40E
5°15'S
Nagada River
Mis Inlet River
Moiro
Wagol River
Gum River
MADANG
KESUP
BILBIL
SEIN
UMUIN
Benir River
Gogol River
Nuru
BISMARCK SEA
LEGEND
Resistivity depth probe
Seismic spread
S1
S2
S3
S4
S5
S6
0 2km
MADANG PNG GEOPHYSICAL SURVEY 1974
LOCALITY MAP
145°40'E
145°45'E
B55/B5-56A

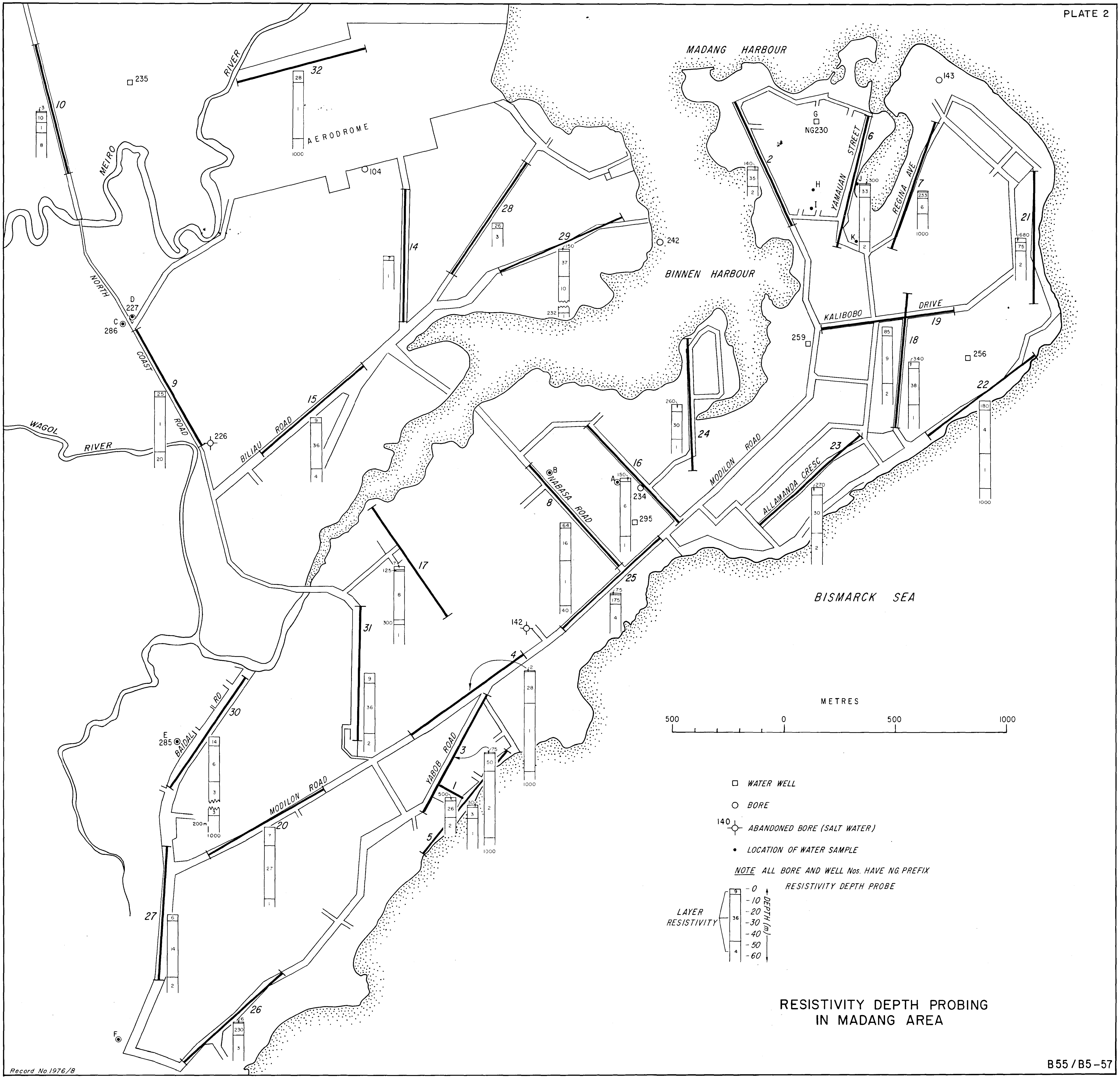

RESISTIVITY DEPTH PROBING IN MADANG AREA

B55/B5-57

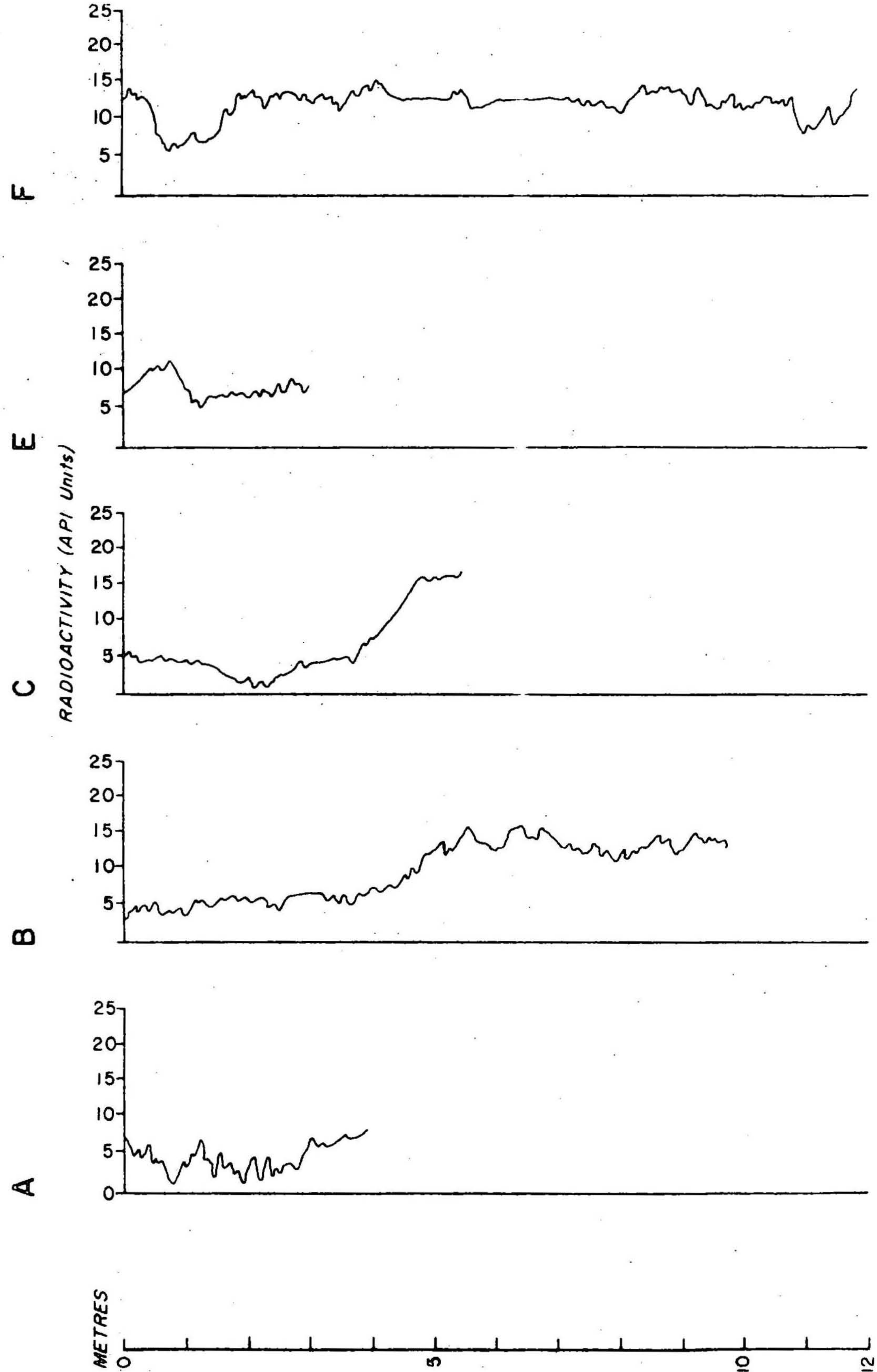

GAMMA RAY LOG
MADANG AREA

RESISTIVITY CURVES DP No.1, DP No.3, DP No.4, DP No.5, DP No.31,

Record No. 1976/8

B55/B5-60

RESISTIVITY CURVES DP No.9, DP No.10, DP No.11, DP No.12, DP No.13, DP No.15, DP No.17

Record No 1976/8

RESISTIVITY CURVES DP No.2, DP No.6, DP No.7, DP No.14, DP No.21, DP No.28, DP No.29, DP No.32

Record No.1976/8

B55/B5-62

RESISTIVITY CURVES DP No.8, DP No.14, DP No.16, DP No.17, DP No.18, DP No.22, DP No.24, DP No.30, DP No.31

○ FIELD MEASUREMENTS

RESISTIVITY MODEL

– – – – – THEORETICALLY CALCULATED RESISTIVITY DEPTH PROBE

RESISTIVITY CURVES DP No.20, DP No.23, DP No.25, DP No.26, DP No.27

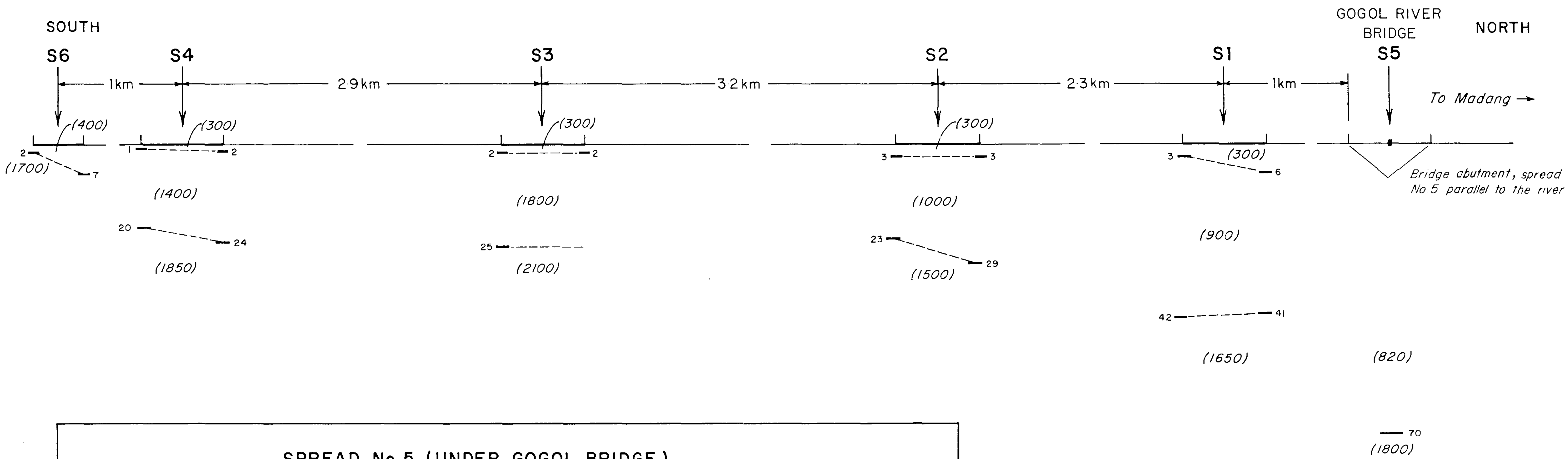

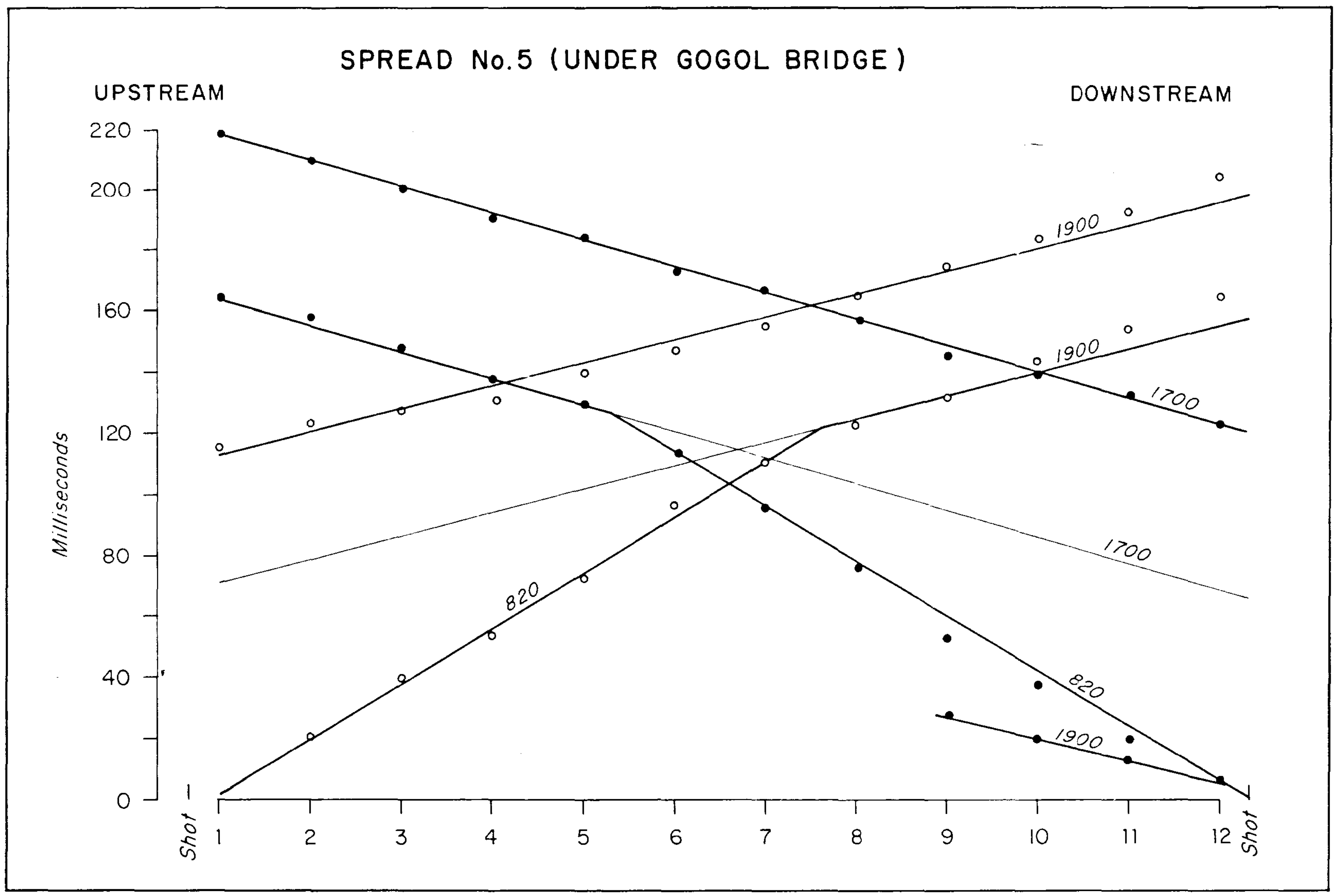

LEGEND

1700	Apparent seismic velocity (m/s)
(1800)	True seismic velocity (m/s)
— 29	Depth to interface (metres)

GOGOL RIVER SEISMIC TEST